DISCHARGE FLOW STUDY OF THE CH_3S+NO_2 REACTION MECHANISM USING $Cl+CH_3SH$ AS THE CH_3S SOURCE

A. MELLOUKI, J.L. JOURDAIN and G. LE BRAS

Centre de Recherches sur la Chimie de la Combustion et des Hautes Températures, CNRS, 45071 Orleans Cedex 2, France

Received 6 April 1988

The discharge flow–EPR–mass spectrometric technique has been used to determine the rate constant for the reaction $Cl+CH_3SH \rightarrow CH_3S+HCl$ (1). We determined $k_1=(1.1\pm0.4)\times10^{-10}$ cm^3 molecule^{-1} s^{-1} at room temperature and at 0.3 Torr. This reaction was found to be a convenient source of CH_3S in discharge flow systems and was used to study the mechanism of the CH_3S+NO_2 reaction. Rate constants were obtained for the reactions $CH_3SO+NO_2 \rightarrow CH_3SO_2+NO$ (4) and $CH_3SO_2+M \rightarrow CH_3+SO_2+M$ (5) giving $k_4=(3\pm2)\times10^{-11}$ cm^3 molecule^{-1} s^{-1} and $k_5\leqslant10$ s^{-1} from modelling the experimental profiles of the reactant and products.

1. Introduction

The organic sulfides CH_3SCH_3 (DMS), CH_3SSCH_3 (DMDS) and CH_3SH (methanethiol) are primarily oxidized in the atmosphere by reactions with OH and NO_3 which have been extensively studied over the last few years [1–5]. For DMS, two recent studies have also suggested that reaction with IO could be an additional sink of DMS in the marine atmosphere [6,7]. Even if the mechanisms of these reactions are not yet fully understood, CH_3S appears to be an important product of the reactions of OH and NO_3 with these sulfur compounds. Further potential oxidation routes of CH_3S in the atmosphere are considered to be reactions with O_2, NO and NO_2. It is therefore of interest to assess their relative importance in order to gain a better knowledge of the atmospheric sulfur cycle and especially the acid deposition process.

Balla et al. [8] have recently measured the rate constants for the reactions of CH_3S with O_2, NO and NO_2 as a function of pressure (1–40 Torr of N_2 or SF_6) and temperature (298–511 K) using the laser photolysis–laser-induced fluorescence technique. Tyndall and Ravishankara [9] have reported rate constant measurements for the reactions of CH_3S with NO_2 and O_2 at 298 K using the same technique. Barnes et al. [10] have recently carried out continuous photolysis experiments together with FTIR analysis of the products for the reaction CH_3S+NO_2 at room temperature in 760 Torr of synthetic air.

The purpose of the present discharge flow study was to gain additional information on the kinetics and mechanisms of the secondary steps of the CH_3S+NO_2 reaction from a quantitative analysis of the products NO and SO_2. We also report a kinetic study of the reaction $Cl+CH_3SH$, which was used as a non-photolytic source of CH_3S.

2. Experimental

The discharge flow–EPR–mass spectrometric apparatus has previously been described [11]. Briefly, a 22 mm inner diameter quartz reactor coated with halocarbon wax (Halocarbon Corp., wax 12.00) equipped with movable inlets is interfaced with a Varian E112 EPR spectrometer using a E235 large access cavity and a Riber QX200 mass spectrometer with effusion sampling of the species through a 100 μm pinhole.

Cl atoms were generated in a side arm or in the sliding injector from a microwave discharge in a Cl_2–He mixture. Cl atoms could be monitored quantitatively by EPR by comparing the spectrum to those of known concentrations of molecular oxygen. The absolute Cl atom concentration was also obtained from a mass-spectrometric titration using the fast reaction $Cl+C_2H_3Br \rightarrow Br+C_2H_3Cl$ and monitoring C_2H_3Br at its molecular peak ($m/e=106$).

The SO_2^+ peak at $m/e=64$ and NO^+ peak at $m/e=30$ were calibrated by flowing known amounts of SO_2 and NO into the reactor. The NO^+ peak was monitored at low electron energy (14 eV) in order to remove the intense signal at the NO^+ peak derived from NO_2. The other peaks were monitored at 23 eV. In a first series of experiments, CH_3SH was introduced through the central injector whereas in a second series, Cl atoms were flowed through the central injector and CH_3SH directly into the reactor in order to avoid recombination of the Cl atoms in the reaction zone.

Gases were stored in 10 ℓ bulbs and diluted with helium. Purities were as follows: methanethiol 99.5%, chlorine 99.5%, NO_2 99.5%, C_2H_3Br 99.5%, NO 99%. They were taken from Matheson cylinders. SO_2 99.9% was supplied by l'Air Liquide. Helium (l'Air Liquide 99.995%) was passed through a liquid nitrogen trap to remove impurities before entering the discharge. The other gases were used without further purification.

3. Results and discussion

3.1. The reaction $Cl+CH_3SH$

This reaction has been chosen to generate CH_3S in our discharge flow reactor according to

$$Cl+CH_3SH \rightarrow CH_3S+HCl\,. \qquad (1)$$

Strong evidence for the predominance of this reaction as opposed to $Cl+CH_3SH \rightarrow CH_2SH+HCl$ was obtained by Dill and Heydtmann [12] on a thermodynamic basis from infrared measurements of the nascent HCl in vibrationally excited states $v=1$ and $v=2$. A branching ratio of unity for reaction (1) was also recently measured [13].

Regarding the kinetics of this reaction, which has never been previously studied, a first series of experiments was carried out by EPR analysis of Cl atoms, CH_3SH being used in excess over Cl. The observed fast decay of Cl atoms and the fairly low sensitivity of EPR detection for Cl atoms (1×10^{11} cm^{-3} for $S/N=1$) did not allow for a precise rate constant measurement for reaction (1) under pseudo-first-order conditions.

Further experiments were carried out under second-order conditions with initial ratios $|Cl|_0/|CH_3SH|_0=0.4$ to 2.7 using mass spectrometry for the analysis of CH_3SH at its molecular peak ($m/e=48$). The total pressure measured in the center of the reaction zone was 0.33 Torr and the mean flow velocity of the gases was 44 m/s. With initial reactant concentrations in the range 1×10^{12}–1×10^{13} cm^{-3}, it was possible to obtain temporal profiles for the reactant and products in the range 0 to 6 ms. A qualitative analysis of the reaction products (fig. 1) led to the detection of the CH_3SCl^+ peak at $m/e=82$. The CH_3S^+ peak also observed was corrected for contributions of CH_3SH measured at its molecular peak ($m/e=48$). Results obtained at $m/e=82$ (CH_3SCl^+) are consistent with the detection of CH_3SCl which would result from the reaction of CH_3S with Cl_2 undissociated in the discharge:

$$CH_3S+Cl_2 \rightarrow CH_3SCl+Cl\,. \qquad (2)$$

It was clear that the chain mechanism (1) + (2) was not suitable for a kinetic study of reaction (1). In order to avoid complications due to the regeneration of Cl atoms, NO_2 was added together with the reactants in fairly high concentrations ($>5\times10^3$ cm^{-3}) so that reaction (2) was unlikely to occur according to the high rate constant reported for the reaction

$$CH_3S+NO_2 \rightarrow CH_3SO+NO \qquad (3)$$

by Balla et al. [8], $k_3=1.09\times10^{-10}$, and Tyndall and Ravishankara [9], $k_3=6.1\times10^{-11}$ at room temperature. Experimentally, the addition of NO_2 led to the disappearance of the CH_3SCl^+ peak with appearance of peaks at $m/e=63$, 30 and 64 corresponding to CH_3SO^+, NO^+ and SO_2^+ (fig. 2).

For the kinetic studies in the presence of NO_2, initial concentrations of CH_3SH were varied from 2.0×10^{12} to 1.0×10^{13} cm^{-3} and initial concentrations of Cl from 1.48×10^{12} to 1.73×10^{13} cm^{-3}. Cl atoms were titrated with C_2H_3Br before and after each experiment. Experimental profiles of CH_3SH as a function of reaction time were compared with those obtained from a computer simulation of the reaction mechanism (table 1) and k_1 was varied in order to

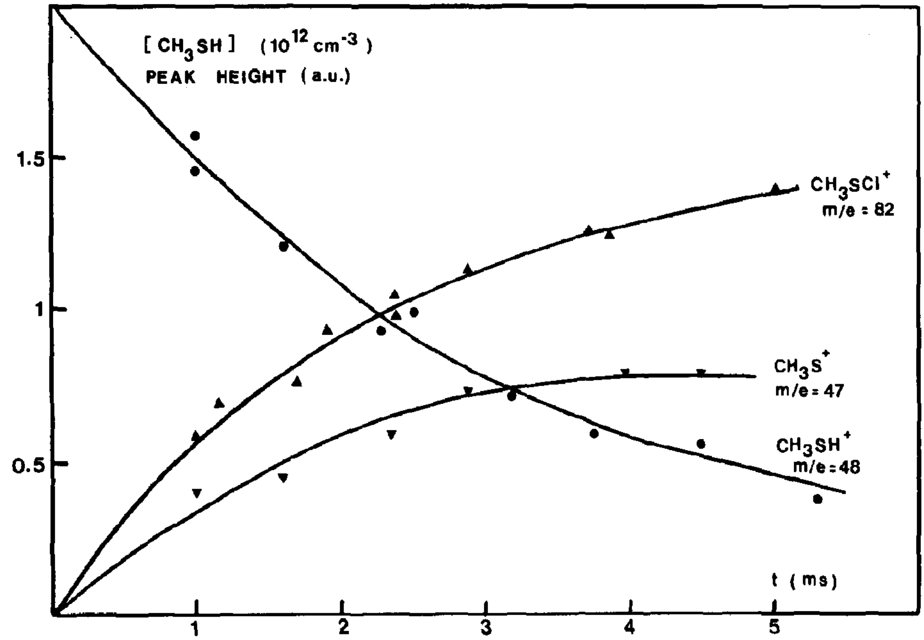

Fig. 1. $Cl+CH_3SH \rightarrow CH_3S+HCl$ (1): profiles as a function of reaction time for the CH_3SH concentration, and the CH_3S^+ and CH_3SCl^+ peak heights, showing the occurrence of the secondary reaction: $CH_3S+Cl_2 \rightarrow CH_3SCl+Cl$ (2) from Cl_2 undissociated in the microwave discharge. Initial concentrations were: $[CH_3SH]_0=2\times10^{12}$, $[Cl]_0=3.2\times10^{12}$ and $[Cl_2]_0=7\times10^{12}$ cm^{-3}.

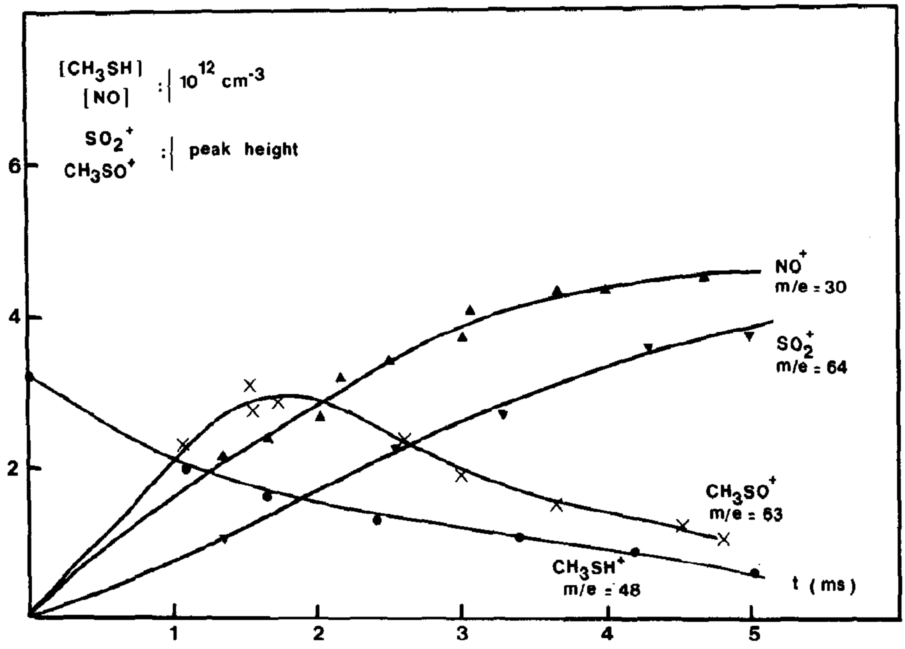

Fig. 2. Reaction system Cl, NO_2, CH_3SH: the profiles of CH_3SH and NO as a function of reaction time are given in absolute concentrations. The SO_2^+ and CH_3SO^+ peaks are given in arbitrary units. Initial concentrations were $[CH_3SH]_0=3.2\times10^{12}$, $[Cl]_0=4.5\times10^{12}$, $[Cl_2]_0=7\times10^{12}$ and $[NO_2]_0=1\times10^{14}$ cm^{-3}.

Table 1

Mechanism used for the computer simulation of the CH_3SH, Cl, Cl_2, NO_2 system at 298 K. Rate constants for reactions (7)–(10) are estimations and are taken from Amano et al. [14]. The rate constant for reaction (11) is taken from Leu [15], that for reaction (6) from the review of Tsang and Hampson [16] and for reaction (12) from Balla et al. [8]

(1)	$Cl+CH_3SH \rightarrow CH_3S+HCl$	k_1
(2)	$CH_3S+Cl_2 \rightarrow CH_3SCl+Cl$	k_2
(3)	$CH_3S+NO_2 \rightarrow CH_3SO+NO$	$(0.61\text{–}1.09)\times10^{-10}$
(4)	$CH_3SO+NO_2 \rightarrow CH_3SO_2+NO$	k_4
(5)	$CH_3SO_2+M \rightarrow CH_3+SO_2+M$	k_5
(6)	$CH_3+CH_3+M \rightarrow C_2H_6+M$	3.5×10^{-11}
(7)	$CH_3+CH_3S+M \rightarrow CH_3SCH_3+M$	2.0×10^{-11}
(8)	$CH_3+CH_3SH \rightarrow CH_3S+CH_4$	2.0×10^{-12}
(9)	$CH_3S+CH_3S \rightarrow CH_3SH+CH_2S$	1.0×10^{-12}
(10)	$CH_3S+CH_3S+M \rightarrow CH_3SSCH_3+M$	1.0×10^{-12}
(11)	$Cl+NO_2 \rightarrow ClONO$	9.3×10^{-15}
(12)	$CH_3S+NO+M \rightarrow CH_3SNO+M$	1.0×10^{-12}

achieve agreement between them. From 23 experiments we obtained

$$k_1=(1.1\pm0.4)\times10^{-10}\ \text{cm}^3\ \text{molecule}^{-1}\ \text{s}^{-1}.$$

Some experiments were also carried out without NO_2 so that reaction (2) was likely to modify the CH_3SH profile, but no variation in k_1 beyond the range of precision was obtained under such conditions. In some experiments without NO_2, NO was added in concentrations high enough to downshift the CH_3SCl^+ profile due to the reaction $CH_3S+NO+M \rightarrow CH_3SNO+M$. Calculations were then carried out to reproduce the modified CH_3SCl^+ profile. From these calculations, it was found that reaction (2) could be given the approximate rate constant $k_2=1\times10^{-12}$ cm^3 molecule^{-1} s^{-1}.

3.2. The reaction CH_3S+NO_2 and subsequent steps

In the experiments described above in which Cl, Cl_2, CH_3SH and NO_2 were flowed together, the profiles of the NO^+ and SO_2^+ peaks were also monitored in addition to the CH_3SH^+ peak. NO^+ and SO_2^+ were calibrated for NO and SO_2 as indicated in section 2. This calibration is justified for NO^+, since this peak is characteristic of NO after correction for the contribution from NO_2. The SO_2^+ peak calibration is described below.

The profiles of CH_3SH^+, NO^+ and SO_2^+ as a function of reaction time were processed on a microcomputer in order to fit the experimental profiles with those obtained from simulation of the reaction mechanism (table 1). The following steps were considered for the oxidation of CH_3S with NO_2:

$$CH_3S+NO_2 \rightarrow CH_3SO+NO, \quad (3)$$

$$CH_3SO+NO_2 \rightarrow CH_3SO_2+NO, \quad (4)$$

$$CH_3SO_2+M \rightarrow CH_3+SO_2+M. \quad (5)$$

Reactions (1), (3), (4) and (5) are the dominant steps in this mechanism.

By adjustments of k_4 and k_5 (table 1) it was usually possible to reproduce the NO^+ profile but not the SO_2^+ profile. Comparison of the experimental and calculated profiles of SO_2^+ suggest that in addition to SO_2, another compound should contribute to this peak. It was assumed that the SO_2^+ peak intensity calibrated for SO_2 alone should be taken as: $SO_2^+=[SO_2]+\alpha[CH_3SO_2]$, where α is the sensitivity of the mass spectrometer for CH_3SO_2 at the SO_2^+ peak, relative to SO_2. With this assumption, we calculated a couple of values (k_5, α) so as to reproduce the SO_2^+ peak profile. A α factor of 0.4–0.5 was usually obtained. In the simulations, the rate constant 6.1×10^{-11} reported by Tyndall and Ravishankara [9] was usually taken for reaction (3) but calculations were also done using the value 1.09×10^{-10} of Balla et al. [8]. Each value is large enough to have no significant effect on the determination of k_4 and k_5. The following values were found for k_4 and k_5:

$$k_4=(3\pm2)\times10^{-11}\ \text{cm}^3\ \text{molecule}^{-1}\ \text{s}^{-1},$$

$$k_5\geqslant10\ \text{s}^{-1}.$$

Additionally for different initial conditions, the ratio $|NO|_{produced}/|CH_3SH|_{reacted}$ for a reaction time of 4–5 ms was found to be in the range 1.5–2. A typical simulation result is shown in fig. 3.

These kinetic and mechanistic data can be compared with previous work. In the laser photolysis–laser-induced fluorescence work reported by Balla et al. [8], the reaction CH_3S+NO_2 was studied as a function of pressure (in the range 1–200 Torr of N_2) and temperature (between 295 and 511 K). Only a small variation of k_3 was noticed with pressure: $k_3=(0.8\pm0.074)\times10^{-11}$ for 1 Torr of N_2 and $k_3=1.06\times10^{-10}$ for 200 Torr of N_2 at 295 K. These authors assumed that the high-pressure limit was obtained for a pressure of 200 Torr and the Arrhenius expression for k_3 was

$$k_3=(8.3\pm1.4)\times10^{-11}\exp[(160\pm120)/RT]\,.$$

No product analysis was carried out and two possible initial channels were suggested by analogy with the similar reactions of CH_3O: $CH_3S+NO_2+M\rightarrow CH_3SNO_2+M$ and $CH_3S+NO_2\rightarrow CH_2S+HONO$. But the essential pressure independence of the rate constant between 1 and 200 Torr of N_2 and the small negative temperature dependence led these authors to propose the following steps: $CH_3S+NO_2\rightarrow CH_3SONO^*\rightarrow CH_3SO+NO$. Therefore, they were unable to unambiguously determine the CH_3S+NO_2 reaction mechanism.

In their FTIR study, when mixtures containing CH_3SSCH_3 and NO_2 were photolysed in N_2 at atmospheric pressure, Barnes et al. [10] found that 2–3 molecules of NO were produced from the photolysis of 1 molecule of CH_3SSCH_3. These results have led these authors to suggest the occurrence of steps (3) and (4). Similar observations and conclusions have been reported by Tyndall and Ravishankara [9] from their laser photolysis–laser-induced fluorescence study. They also found a yield of 2 molecules of NO produced per CH_3S reacted and they obtained $k_3=(6.1\pm0.5)\times10^{-11}$ at 298 K. Our value obtained by a different method also supports the above mechanism, in agreement with these two recent studies. These data also yield the first determination of k_4.

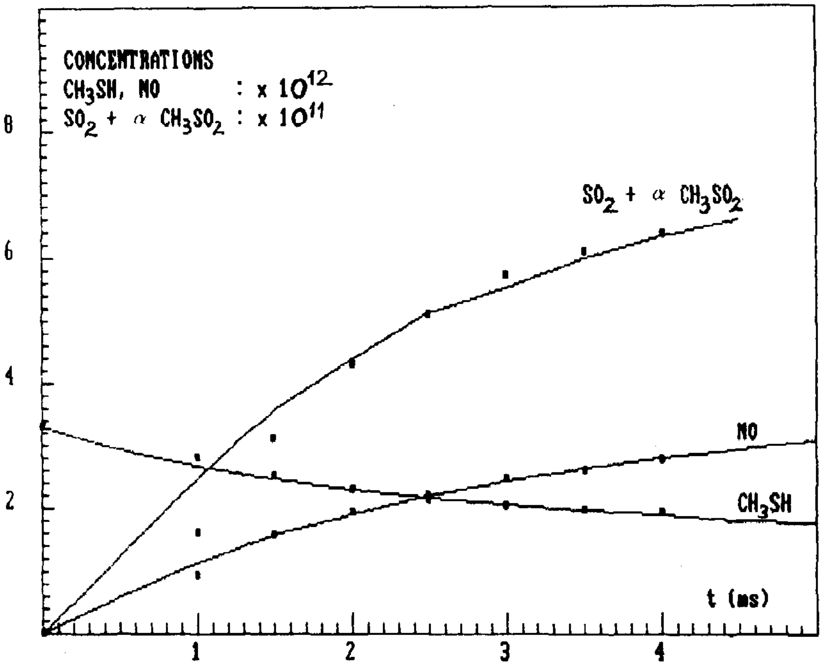

Fig. 3. Result of a simulation run under the following initial conditions: $[CH_3SH]_0=3.27\times10^{12}$, $[Cl]_0=2.09\times10^{12}$ and $[NO_2]_0=2.16\times10^{14}$ cm^{-3}. Solid lines are the calculated curves and the dots represent the experimental data. α (see text) was found to be 0.43, $k_1=1.07\times10^{-10}$, $k_4=5\times10^{-11}$ cm^3 molecule^{-1} s^{-1} and $k_5=10$ s^{-1}.

Reaction (5) was mentioned by Barnes et al. [10] to explain the formation of SO_2 in their experiments. They found SO_2 yields of 38 and 46% per CH_3S reacted in 760 Torr of N_2 and in synthetic air, respectively. Even if no rate data are given in their study, the observation of SO_2 may be consistent with our k_5 measurement, if we consider the higher reaction times of their study (120 to 600 s instead of less than 10 ms in our work) and higher pressure (760 Torr compared to 0.3 Torr) because we can expect that k_5 is pressure dependent.

Our k_5 measurement can also be compared with the results obtained by Good and Thynne [17], who considered reaction (5) as the reverse step of the reaction $CH_3+SO_2+M \rightarrow CH_3SO_2+M$. They used a pressure of 50 Torr and a temperature range 298–437 K and obtained $k_5(s^{-1})=1\times10^{13}\times\exp(-22400/RT)$. Their activation energy is markedly higher than the estimate of 17.2 kcal/mole given by Horowitz [18] from a study of the radiolytic decomposition of methanesulfonic chloride in the liquid phase. This last value is in good agreement with the thermochemical determination of 18 kcal/mole reported by Benson [19]. If we assume a pre-exponential factor of 1×10^{13} as given by Good and Thynne, our upper limit of 10 s^{-1} for k_5 would correspond to a lower limit of 16.5 kcal/mole for the activation energy. This estimate is consistent with the value of Horowitz and Benson.

In conclusion, this work shows that in flow reactors, the reaction $Cl+CH_3SH$ is a suitable source of the CH_3S radical and its rate constant was measured. From a computer analysis of CH_3SH^+, CH_3SO^+, NO^+ and SO_2^+ peak profiles and using the rate constants reported for the reaction CH_3S+NO_2, a value was obtained for the rate constant of reaction (4). The decomposition rate of CH_3SO_2 was not important at low pressure and the SO_2^+ peak was mainly representative of CH_3SO_2.

For atmospheric applications, the present study confirms that the CH_3S+NO_2 reaction can be an important oxidation route of CH_3S with NO_2 concentrations at ppb levels or lower. The actual importance of this reaction will depend on the rate constant for the reaction CH_3S+O_2, for which an upper limit of 3×10^{-18} at 298 K [9] is currently the best estimate. The present determination of the rate constant for the reaction CH_3SO+NO_2 indicates that this reaction is also of potential atmospheric importance. This will depend on possible alternate oxidation routes of CH_3SO, for instance by O_2 and O_3, which are presently unknown. Finally, these results should contribute to a better understanding of the chemical transformation of some organic sulfides in the atmosphere and to the evaluation of their SO_2 yields.

Acknowledgement

The authors thank Professor K.H. Becker and his co-workers, Dr. Ravishankara and Dr. Tyndall for communicating their results prior to publication.

References

[1] D. Martin, J.L. Jourdain and G. Le Bras, Intern. J. Chem. Kinetics 17 (1985) 1247, and references therein.

[2] R. Atkinson, Chem. Rev. 86 (1986) 69, and references therein.

[3] H. MacLeod, S.M. Aschmann, R. Atkinson, E.C. Tuazon, J.A. Sweetman, A.M. Winer and J.N. Pitts Jr., J. Geophys. Res. 91 (1986) 5338.

[4] G.S. Tyndall, J.P. Burrows, W. Schneider and G.K. Moorgat, Chem. Phys. Letters 130 (1986) 463.

[5] J. Heicklen, Rev. Chem. Intermediates 6 (1985) 175.

[6] D. Martin, J.L. Jourdain, G. Laverdet and G. Le Bras, Intern. J. Chem. Kinetics 19 (1987) 503.

[7] I. Barnes, K.H. Becker, P. Carlier and G. Mouvier, Intern. J. Chem. Kinetics 19 (1987) 489.

[8] R.J. Balla, H.H. Nelson and J.R. McDonald, Chem. Phys. 109 (1986) 101.

[9] G.S. Tyndall and A.R. Ravishankara, in: Proceedings of the Symposium Biogenic Sulfur in the Environment, 194th ACS Meeting, New Orleans (August/September 1987) p. 421; to be published in ACS Monograph Series (1988).

[10] I. Barnes, V. Bastian, K.H. Becker and H. Niki, Intern. J. Chem. Kinetics, to be published.

[11] J.L. Jourdain, G. Le Bras and J. Combourieu, J. Phys. Chem. 85 (1981) 655.

[12] B. Dill and H. Heydtmann, Chem. Phys. 35 (1978) 161.

[13] G.S. Tyndall, private communication.

[14] A. Amano, M. Yamada, K. Ashimoto and K. Sugiura, Nippon Kagaku Kaishi 3 (1983) 385.

[15] M.T. Leu, Intern. J. Chem. Kinetics 16 (1984) 1311.

[16] W. Tsang and R.F. Hampson, J. Phys. Chem. Ref. Data 15 (1986) 1168.

[17] A. Good and J.C.J. Thynne, Trans. Faraday Soc. 63 (1967) 2708.

[18] A. Horowitz, Intern. J. Chem. Kinetics 8 (1976) 709.

[19] S.W. Benson, Chem. Rev. 78 (1978) 23.